Supplement 1
NEDO-10527
72NED57
CLASS I
July 1972

ROD DROP ACCIDENT ANALYSIS FOR LARGE BOILING WATER REACTORS ADDENDUM NO. 1 MULTIPLE ENRICHMENT CORES WITH AXIAL GADOLINIUM

R. C. Stirn
C. J. Paone
R. M. Young

Technical Contributions by:

J. M. Haun
L. C. Jansen

Approved: L. K. Holland
L. K. Holland, Manager
Systems Engineering

ATOMIC POWER EQUIPMENT DEPARTMENT • GENERAL ELECTRIC COMPANY
SAN JOSE, CALIFORNIA 95114

GENERAL ELECTRIC

NOTICE

TABLE OF CONTENTS

LIST OF ILLUSTRATIONS

ABSTRACT

This Report is an Addendum to NEDO-10527 (1) and supplements the parametric results presented previously to include Browns Ferry and Zimmer class product line boiling water reactors (BWR's) which employs the design concepts of axial gadolinium for power shaping and multiple enrichment fuel bundles.

1. INTRODUCTION

This report presents the rod drop accident results for the Browns Ferry and Zimmer class product line boiling water reactors (BWR's) which employ the use of axial gadolinium for power shaping and multiple enrichment fuel designs. The mathematical methods which were used for this study were previously discussed in detail in NEDO-10527 (1) and will not be presented here; however, the pertinent data used for this analysis (i.e., the geometry considerations, the scram reactivity function, the accident or control rod reactivity function, and the total control rod worth) and changes in the application of the numerical methods are presented when relevant.

The rod drop accident results presented in this supplement were generated for the beginning of life condition. At this time, it is anticipated that the accident consequences will become less severe as core exposure increases. The reasons for these reduced accident consequences are the increase in the Doppler feedback due to Pu-240 buildup [approximately 20% increase at end of cycle (2)] and the reduction in the accident reactivity insertion rates and the increase in the scram insertion rates as the gadolinium depletes.

2. PARAMETRIC RESULTS OF ROD DROP ACCIDENT

2.1 GENERAL COMMENTS

From these results it will be seen that the rod drop accident is slightly more severe than was presented in NEDO-10527. However, if in-sequence control rod patterns are maintained the peak fuel enthalpy will always be less than the design limit of 280 cal/gm. Qualitatively this shift in the results can be attributed to the three major factors listed below:

1. The multiple enrichment design concept results in higher local peaking factors than were previously observed in single enrichment designs at the cold and hot startup reactor states. For the cold and hot startup reactor states, the local peaking factors were 1.44 and 1.36 respectively, for the multiple enrichment design; whereas, these values were typically 1.24 for previous single enrichment BWR designs.

2. As will be seen in Section 3.4, the accident reactivity insertion rate is increased due to the use of axial gadolinium for power shaping.

3. As will be seen in Section 3.5, the scram reactivity insertion rate is decreased due to the use of gadolinium for power shaping.

   Aside from the slight increase in the severity of the results, the trends which were observed for the BWR designs using uniform curtains for temporary control augmentation generally apply to the designs employing multiple enrichment with axial gadolinium.

2.2 RESULTS OF THE ROD DROP EXCURSION IN THE STARTUP RANGE

The results of the rod drop accident for the cold and hot startup reactor operating states are shown parametrically in Figures 2-1 and 2-2 respectively. The general trends observed for these results were identical to those observed and discussed in NEDO-10527.

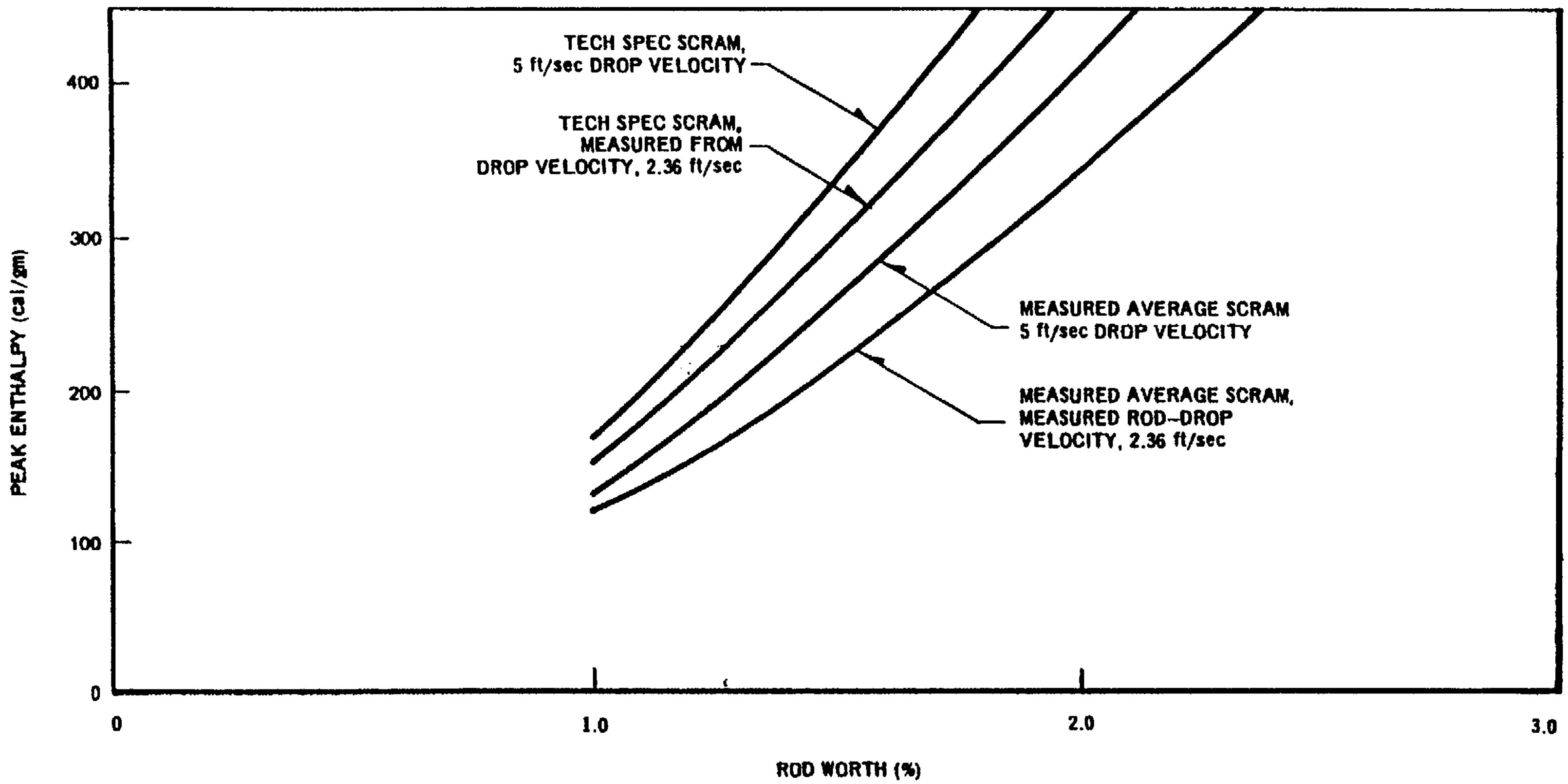

Figure 2-1. Peak Fuel Enthalpy as a Function of Control Rod Worth, Rod Drop Velocity, and Scram Insertion Rate for the Cold Startup Operating State

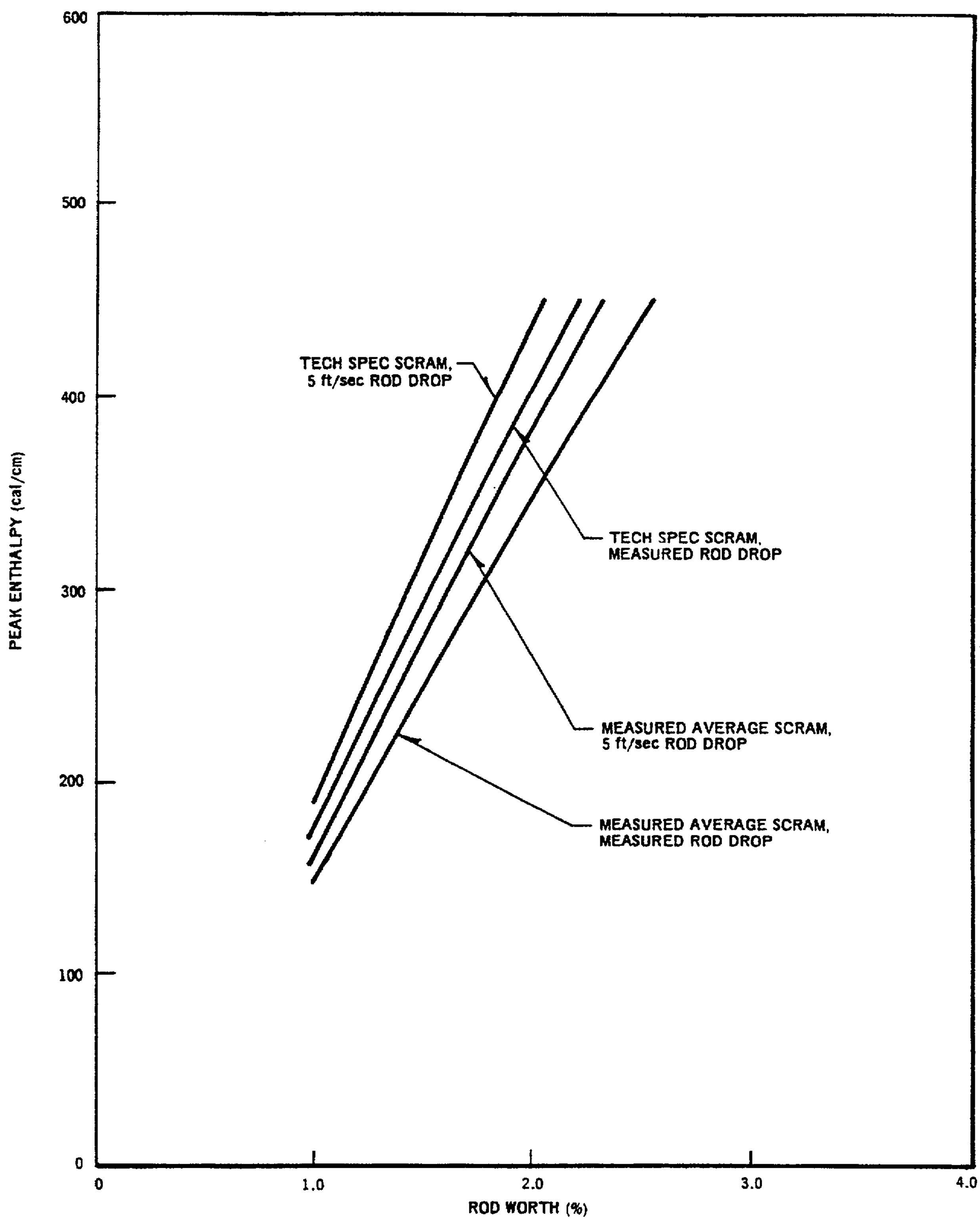

Figure 2-2. Peak Fuel Enthalpy as a Function of Control Rod Worth, Rod Drop Velocity, and Scram Insertion Rate for the Hot Startup Operating State

In addition to general trends, it is observed that the severity of the rod drop accident has increased somewhat for the 5 fps rod drop velocity and Technical Specification scram times (e.g., a 1.36% rod yields 280 cal/gm for the cold startup condition whereas a 1.6% rod yielded 280 cal/gm previously in NEDO-10527). This is almost entirely due to the three effects discussed in Section 2.1 above.

It is also observed that the sensitivity of the results to the rod drop velocity and scram insertion rates is greatly reduced. This can be seen better by comparison of Figure 2-3 to Figure 3-9 of NEDO-10527. These trends are primarily due to items 2 and 3 of Section 2.1.

2.3 RESULTS OF THE ROD DROP EXCURSION IN THE POWER RANGE

The results of the rod drop accident at 10% of rated power are less severe than those for the hot startup reactor state. The reasons for this trend were discussed previously in Section 3.3 of NEDO-10527. However, the peak fuel enthalpy for a 2.0% control rod dropped from 10% power at 5 ft/sec (using Technical Specification scram insertion times) was calculated to be 397 cal/gm. This is significantly higher than the 172 cal/gm value calculated for the fuel design employing uniform curtains for a 3.1% control rod at the same conditions. This trend observed for the cores employing multiple enrichment and axial gadolinia can be attributed to the phenomenon discussed in Sections 2.1, 3.4, and 3.5 of this report.

2.4 SUMMARY OF ROD DROP EXCURSION RESULTS

The best perspective of the rod drop accident at beginning of life is demonstrated by Figure 2.4. The following conclusions can be made concerning these results assuming Technical Specification scram rates and a 5 fps rod drop velocity:

(1) Rod drop accidents involving in-sequence control rods (no operator errors) will always result in peak fuel enthalpies less than 280 cal/gm;

(2) Above a moderator density of 0.91 gm/cc (~ 160°C), rod drop accidents involving maximum worth rods developed due to the worst single operator error will always result in peak fuel enthalpies less than 280 cal/gm; and

(3) Above 20% power, even multiple operator errors will not produce rod worths large enough to exceed fuel enthalpies of 280 cal/gm.

In addition. Figure 2-4 demonstrates that single operator errors will result in peak fuel enthalpies less than 280 cal/gm if measured scram insertion rates and rod drop velocities are employed when doing the analyses at beginning of life.

These results also indicate that bypassing or shutting down the rod worth minimizer above 10% of rated power is most conservative since above ~ 160°C, peak fuel enthalpies will always be less than 280 cal/gm (assuming the worst single operator error).

In addition to presenting these results for the beginning of life (BOL) condition, the rod drop accident results calculated at BOL have been combined with the maximum control rod worths at the most reactive point in the operating cycle (6500 MWd/T). These results are plotted in Figure 2-3, and definitely represent a worst case condition since it combines the worst conditions for the rod drop accident with the worst conditions for the maximum rod worth. As discussed previously, the rod drop accident results will become less severe with increasing exposure due to the increased Doppler feedback with the accumulation of Pu-240 and also due to the fact that both the accident and scram reactivity shape function characteristics will become more favorable as gadolinia depletion occurs. Even for these worst case conditions, Figure 2-3 substantiates the following conclusions:

(1) Rod drop accidents involving in-sequence control rods (no operator errors) will always result in peak fuel enthalpies less than 280 cal/gm; and

(2) Above 5% of rated power, rod drop accidents involving maximum worth rods developed due to the worst single operator error will always result in peak fuel enthalpies less than 280 cal/gm; therefore, it will be conservative to bypass the rod worth minimizer above 10% of rated power since peak fuel enthalpies will always be less than the design limit of 280 cal/gm (assuming the worst single operator error).

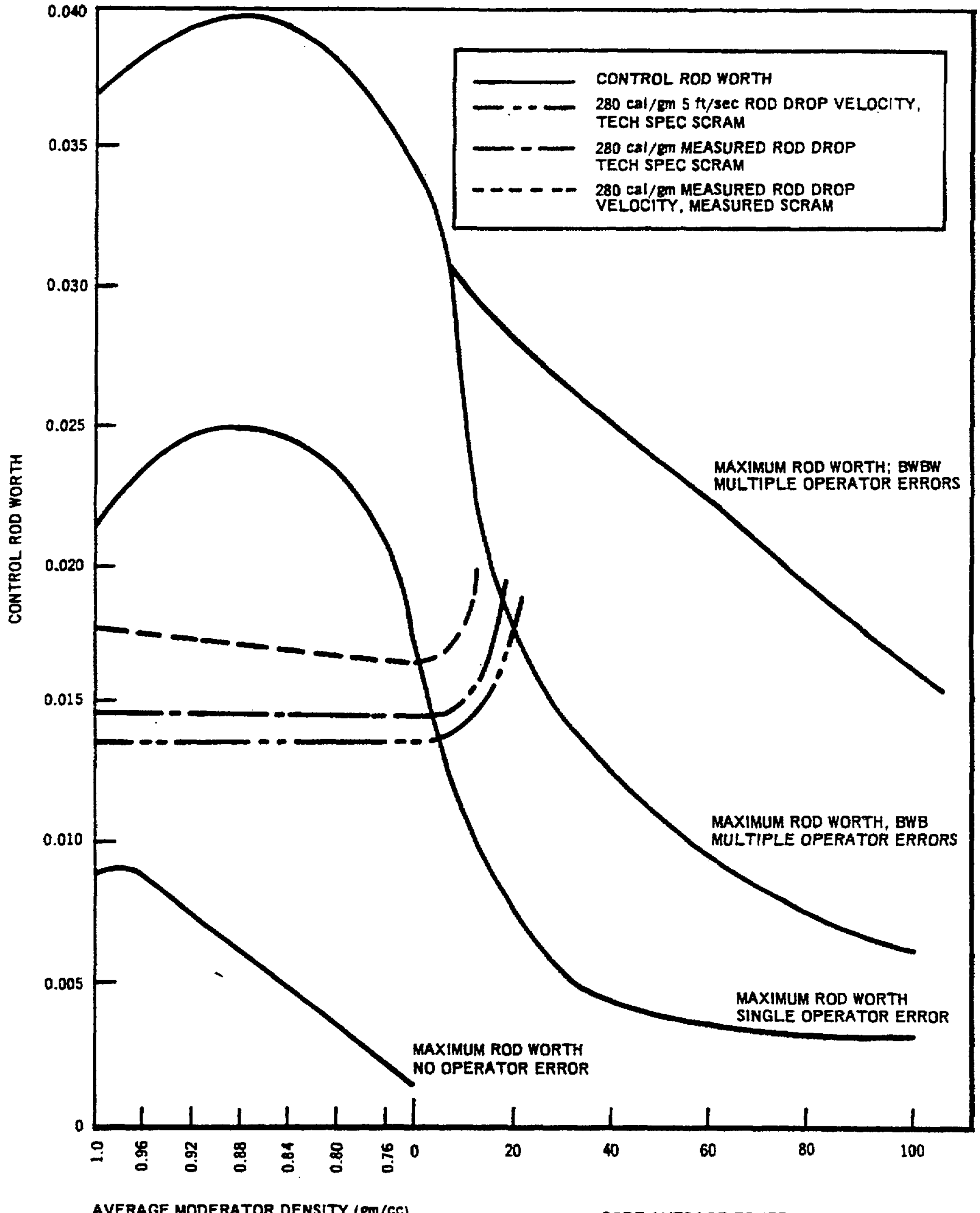

Figure 2-3. Parametric Results of Rod Drop Accident (6500 MWd/T Rod Worth Curves, BOL Rod Drop Accident Results)

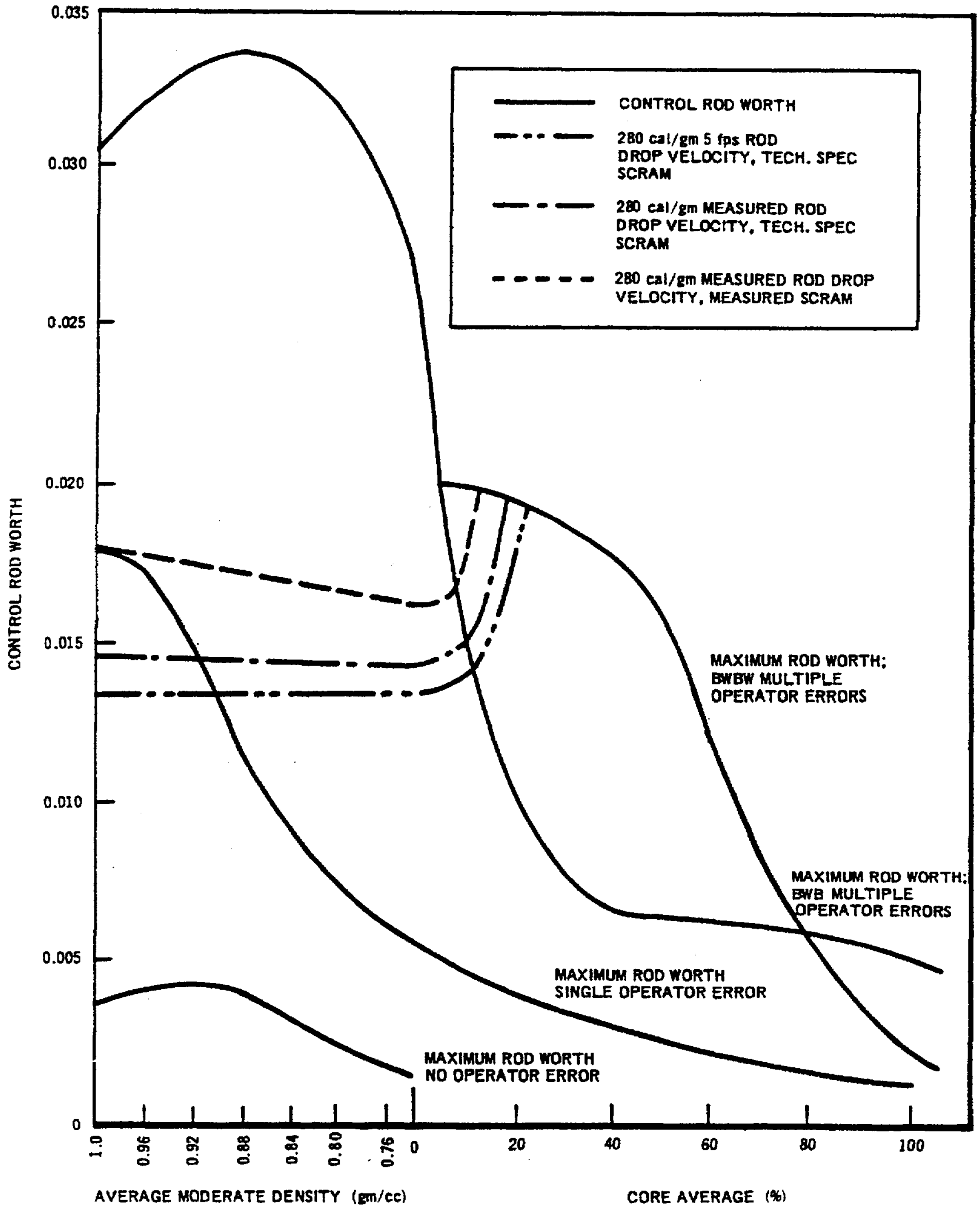

Figure 2-4. PARAMETRIC RESULTS OF ROD DROP ACCIDENT (BOL)

3. METHOD OF ANALYSIS

3.1 INTRODUCTION

The mathematical methods which were used to analyze the rod drop accident for Browns Ferry and Zimmer class product line reactors employing axial gadolinium for power shaping are identical to those discussed in NEDO-10527 and will not be reiterated here. However, due to the use of the multiple enrichment and axial gadolinium concepts the application of the numerical methods has changed such that these spatial effects are properly accounted for. These changes along with pertinent results are discussed below.

3.2 GENERATION OF NUCLEAR CONSTANTS

The nuclear constants (i.e., cross sections, average neutron speeds, delayed neutron fractions, etc.) and the local peaking factors were calculated using the standard lattice design techniques as described in the PSAR's and FSAR's and will not be discussed here in detail. In the case of the single enrichment design discussed in NEDO-10527, the nuclear constants were generated using single bundle calculations; however, for the multiple enrichment design being discussed in this report, the nuclear constants were generated using four bundle calculations performed using two-dimensional XY geometry with the fuel pins, in-channel moderator, channel, gap water, and control blade being discretely represented.

Since the nuclear constants are homogenized over the four bundles and the local peaking factors are normalized over the four bundles, the bundle power mismatch and neutron leakage effects between the high and low enriched bundles are properly accounted for using the approach described above. These homogenized nuclear constants are then used in the RZ geometry described below for analyzing the rod drop accident.

3.3 GEOMETRY FOR ANALYZING ROD DROP ACCIDENT

The geometry for analyzing the rod drop accident is slightly more complex for those designs which employ axial gadolinium for power shaping. This is further complicated by the fact that the axial gadolinium shaping varies radially. The bundle loading pattern and the axial gadolinium distribution in the various core regions are shown in Figures 3-1 through 3-3 for a typical Browns Ferry and Zimmer class product line BWR which employs the multiple enrichment and axial gadolinium concepts. As can be observed from these figures, the low and high enriched bundles can be represented by four bundle modules as discussed in Section 3.2, and the axial gadolinium distribution is zoned radially.

The geometry as depicted by Figures 3-1 through 3-3 was reduced to two-dimensional RZ geometry by homogenization of the four bundle module as described in Section 3.2 and conservation of volume. Therefore, when analyzing the rod drop accident for a center control rod, the geometry as shown by Figure 3-4 will accurately represent the reactor core and all spatial effects.

When analyzing the rod drop accident in the power range, an uncontrolled region on the periphery of the reactor core is added to represent the BWBW* geometry which is used for analyzing the accident at this reactor state. In addition, the reactor core is subdivided into annular and 24 axial zones such that the radial and axial void distribution can be accurately represented. The actual void distribution is calculated using a three-dimensional coupled nuclear-thermal-hydraulics calculation.

3.4 ACCIDENT REACTIVITY SHAPE FUNCTION

With the exception of the geometry effects discussed in Section 3.3, the methods used for calculating the accident reactivity shape functions were identical to those described in Section 7.3 of NEDO-10527 (1). The results of these analyses are shown by Figures 3-5 through 3-7 for the cold-startup, hot-startup, and hot-standby cases, respectively. When comparing these results to Figures 7-3 through 7-5 of NEDO-10527, it will be noted that the accident shape function for the axial gadolinium cores has a steeper slope, and also that the accident shape function is relatively independent of the total rod worth. This is due primarily to the effects of the axial gadolinium.

The most significant change was observed between the accident shape functions for the hot-standby operating state. This is due primarily to two separate effects. The first and most obvious is the effect of the axial gadolinium shaping. The second effect is more complex and requires additional explanation.

* B - denotes controlled fuel
W - denotes uncontrolled fuel

In order to achieve the desired axial power shaping, more gadolinium was added to the core than was required to meet reactivity shutdown requirements. This resulted in a reactor which has a low excess reactivity at beginning of life (BOL). Due to this low excess reactivity, the outer uncontrolled region of the BWBW geometry which is used to analyze the rod drop accident at hot-standly must be relatively large to maintain a critical reactor. Therefore, the power and, hence, voids in this outer region are relatively high, whereas the power and voids in the central uncontrolled region surrounding the center or accident control rod are low. Since the geometry selected for this analysis results in a highly decoupled system neutronically, the formation of voids in the outer region has very little influence on the accident shape function of the center control rod. As can be seen by comparison of Figures 3-6 and 3-7, this phenomenon results in an accident shape function very close to that for the hot-startup condition.

It should be emphasized here that the BWBW geometry used for the hot-standby analysis is highly abnormal and bears no resemblance to a normal control rod withdrawal sequence. Hence, this pattern could only be established with multiple operator errors. With normal withdrawal sequences during startup, the void distribution even with the worst single operator error will be uniformly distributed. Therefore, the rod shape and scram functions will have much flatter slopes, and the rod drop accident in the power range will be of little consequence.

3.5 SCRAM REACTIVITY SHAPE FUNCTION

With the exception of the geometry effects discussed in Section 3.3, the methods used for calculating the scram reactivity shape functions were identical to those described in Section 7.4 of NEDO-10527 (1). The results of these analyses are shown by Figures 3-8 through 3-10 for the cold-startup, hot-startup, and hot-standby conditions, respectively. When comparing these results to Figures 7-6 and 7-7 of NEDO-10527, it will be noted that the scram response for the axial gadolinium cores will be slower.

As was the case for the accident shape function, this phenomenon is primarily due to the effects of axial gadolinium. It should also be noted that the total scram reactivity worth is significantly higher for reactors employing axial gadolinium. As stated previously in Section 3.4, the amount of gadolinium required to achieve the desired power shaping effects reduces the amount of excess reactivity significantly; therefore, more control rods must be withdrawn to achieve criticality. This in turn increases the total scram worth since a greater number of control rods will be inserted upon receipt of the scram signal.

3.6 CONTROL ROD WORTH CALCULATIONS

3.6.1 Control Rod Worth in Startup Range

The same basic methods as discussed in Section 7.6.2.1 of NEDO-10527 were used to evaluate the maximum in-sequence and out-of-sequence control rod worths in the startup range. However, to properly account for the effects of multiple enrichment and axial gadolinium design, concepts, certain modifications to the design procedures were required.

In order to accommodate the multiple enrichment design, the three-group homogenized cross sections to be used in the XY diffusion theory calculation were generated over four bundle modules for fuel with 3, 4, and 5 gadolinium pins as discussed in Section 3.2. The homogenized cross sections obtained from these calculations were then entered into a one-dimensional, three-group slab diffusion theory calculation to axially average the cross sections and to obtain the transverse leakage or buckling effects. These averaged cross sections and transverse bucklings were then input into the XY diffusion theory calculations. This method is basically a synthesis technique which represents the three-dimensional effects of the problem.

3.6.2 Control Rod Worths in the Power Range

Since either RZ or XYZ calculations were used to calculate the control rod worths in the power range as discussed in Section 7.6.2.2 of NEDO-10527, all spatial effects will be properly accounted for. Therefore, in the power range the methods discussed in NEDO-10527 were used to calculate the maximum control rod worths.

3.6.3 Results of Analysis

The current class of reactors being designed with the multiple enrichment fuel and axial gadolinium obviously have some operating characteristics which vary from previous BWR designs which used uniform curtains for temporary control augmentation. One of these characteristics is that the excess reactivity increases with exposure to some point in the operating cycle and then decreases. For designs being considered in this report, the maximum excess reactivity occurs at a core average exposure of approximately 6,500 MWd/T. From studies it has also been determined that the maximum control rod worth will occur at the point of maximum excess reactivity. This conclusion also follows logically from the fact that this excess reactivity must be controlled by the movable control system; therefore, more control rods must be inserted and a more heterogeneous control rod pattern results which in turn will have the tendency to increase rod worth.

The phenomenon described above can be seen by comparing the maximum control rod worth curves for multiple errors at 6,500 and 0 MWD/T core average exposures as shown by Figures 3-11 and 3-12 respectively. By comparing these results it is seen that the rod worth curves at 6,500 MWd/T have shifted upward and to the right. Beyond exposures of 6,500 MWd/T, the core excess reactivity decreases and the rod worth curve will shift downward and to the left. Therefore, the worst case condition from the standpoint of control rod worth will occur at a core average exposure of approximately 6,500 MWd/T.

By comparing Figure 3-11 to Figure 7-15 of NEDO-10527, it will be noted, with the exception of the maximum in-sequence rod worth, that the maximum control rod worths are slightly less. This is primarily due to the fact that the excess reactivity for the gadolinium cores at 6,500 MWd/T was less than that for the curtain cores at BOL, which was the most reactive point in the cycle for the particular fuel design analyzed in NEDO-10527.

3.7 SCRAM BANK INSERTION RATES

In addition to parameterizing the control blade drop velocity, the scram insertion rate was also varied. The maximum scram insertion times used in this study were the Technical Specification values, and the minimum insertion times employed were experimentally measured values. The experimental average insertion times measured from the de-energization of the scram solenoid valves to the 90% insertion points were 1.6 and 2.6 sec for the cold and hot startup conditions, respectively.

Since Technical Specification scram times must be employed when doing safeguards analyses, no attempt will be made to justify the measured scram insertion times. The reason for including the measured scram times in this study was merely to demonstrate both the rod drop accident results under expected or realistic conditions and also the sensitivity of the accident to scram insertion rates.

The Technical Specification scram rates which were used in this analysis are tabulated below. The zero point in time for these specifications is the point of the de-energization of the scram solenoid valves. Therefore, all delay times except the instrument delay times associated with the APRM system scram circuitry are included in the Technical Specifications. An instrument delay time of 90 msec was used for this study including those results obtained using the measured scram times.

PERCENT OF ROD INSERTION	TIME FROM DE-ENERGIZATION OF SCRAM SOLENOID VALVE (SEC)
5%	0.475
20%	1.10
50%	2.0
90%	5.0

3.8 DOPPLER REACTIVITY FEEDBACK MODEL

The Doppler reactivity feedback was calculated using the same methods discussed in Section 7.7 of NEDO-10527 with the exception of performing the lattice calculations using a four bundle module rather than a single fuel bundle as discussed previously in Section 3.2. The Doppler coefficients for this fuel design are given in Reference 2.

J \ I	1	2	3	4	5	6	7	8	9	10	11	12	13	14	15	16	17	18	19	20	21	22	23	24	25	26
1										3	3	3	3	3	3	3	3									
2								3	3	3	3	1	3	3	3	1	3	3	3							
3					3	3	3	1	1	3	3	1	1	3	3	1	1	3	1	3	3	3				
4				3	3	3	3	3	3	2	2	2	2	2	2	2	3	3	3	3	3	3	3			
5				3	3	3	3	2	2	2	2	2	2	2	2	2	2	2	2	3	3	3	3			
6			3	3	1	2	2	1	1	2	2	1	1	2	2	1	1	2	2	1	1	3	3	3		
7			3	1	1	2	2	1	1	2	2	1	1	2	2	1	1	2	2	1	1	3	3	3		
8		3	3	3	2	2	2	2	2	2	2	2	2	2	2	2	2	2	2	2	2	2	3	1	3	
9		3	3	3	2	2	2	2	2	2	2	2	2	2	2	2	2	2	2	2	2	2	3	3	3	
10	3	3	3	1	1	2	2	1	1	2	2	1	1	2	2	1	1	2	2	1	1	2	2	1	3	3
11	3	1	3	1	1	2	2	1	1	2	2	1	1	2	2	1	1	2	2	1	1	2	2	1	1	3
12	3	3	3	2	2	2	2	2	2	2	2	2	2	2	2	2	2	2	2	2	2	2	2	3	3	3
13	3	3	3	2	2	2	2	2	2	2	2	2	2	2	2	2	2	2	2	2	2	2	2	3	3	3
14	3	1	3	1	1	2	2	1	1	2	2	1	1	2	2	1	1	2	2	1	1	2	2	1	3	3
15	3	3	3	1	1	2	2	1	1	2	2	1	1	2	2	1	1	2	2	1	1	2	2	1	1	3
16	3	3	3	2	2	2	2	2	2	2	2	2	2	2	2	2	2	2	2	2	2	2	2	3	3	3
17	3	3	3	2	2	2	2	2	2	2	2	2	2	2	2	2	2	2	2	2	2	2	2	3	3	3
18		3	3	1	1	2	2	1	1	2	2	1	1	2	2	1	1	2	2	1	1	2	3	1	3	
19		3	3	1	1	2	2	1	1	2	2	1	1	2	2	1	1	2	2	1	1	2	3	1	3	
20			3	3	3	2	2	2	2	2	2	2	2	2	2	2	2	2	2	2	2	3	3	3		
21			3	3	3	2	2	2	2	2	2	2	2	2	2	2	2	2	2	2	2	3	3	3		
22				3	1	3	3	1	1	2	2	1	1	2	2	1	1	2	2	1	1	3	3			
23				3	3	3	3	1	1	2	2	1	1	2	2	1	1	3	3	1	3	3	3			
24					3	3	3	3	3	3	3	3	3	3	3	3	3	3	3	3	3	3				
25								3	3	3	3	3	1	3	3	1	3	3	3							
26										3	3	3	3	3	3	3	3									

BUNDLE DESCRIPTION

TYPE	ENRICHMENT
1	1.1
2	2.5
3	2.5

TYPE

1 = 117 ASSEMBLIES
2 = 252 ASSEMBLIES
3 = 179 ASSEMBLIES

Figure 3-1. Fuel Bundle Loading Pattern (see Figures 3-2 and 3-3 for Axial Gadolinium Distribution)

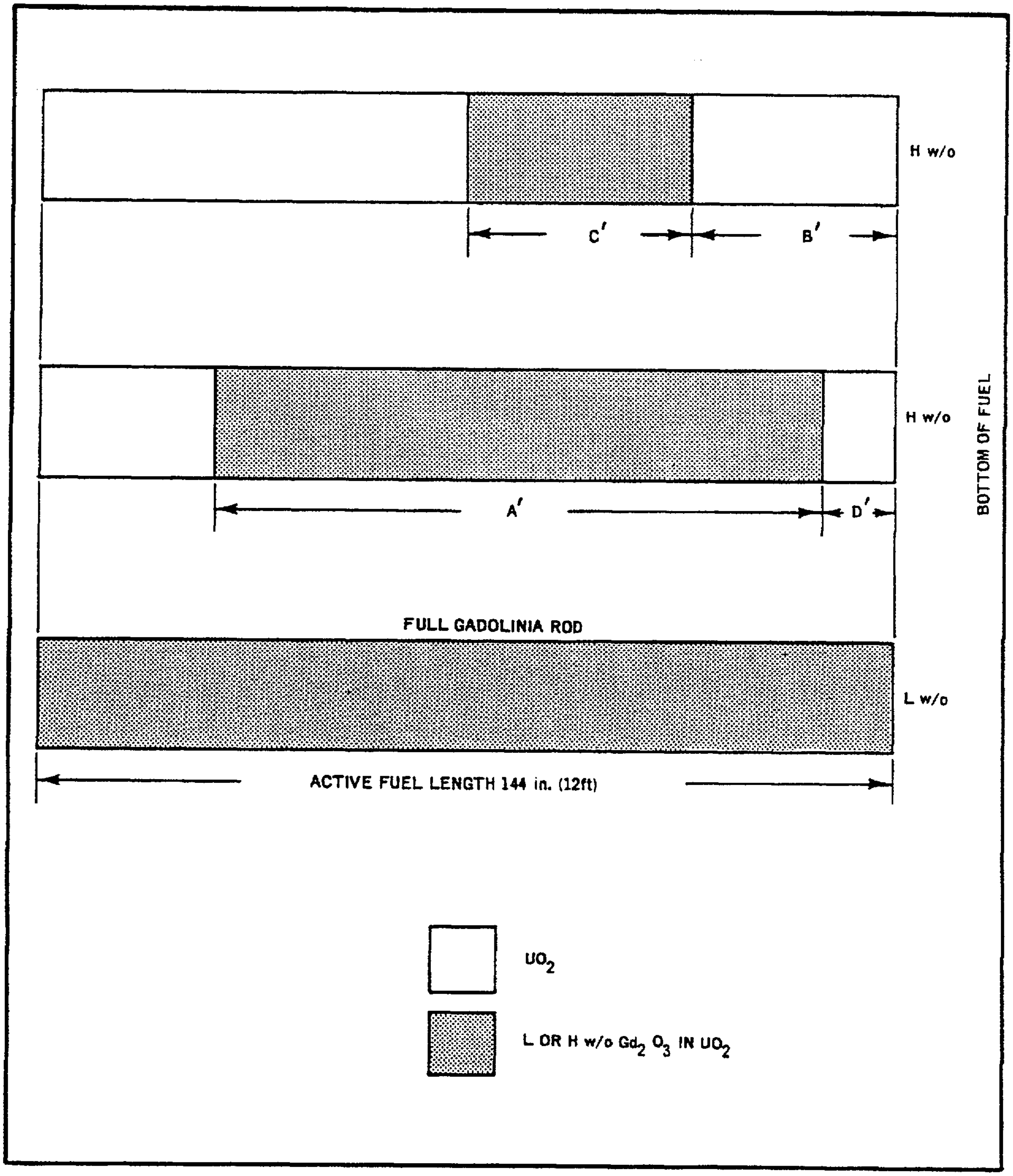

Figure 3-2. Axial Gadolinium Distribution for Bundle Type 2 of Figure 3-1.

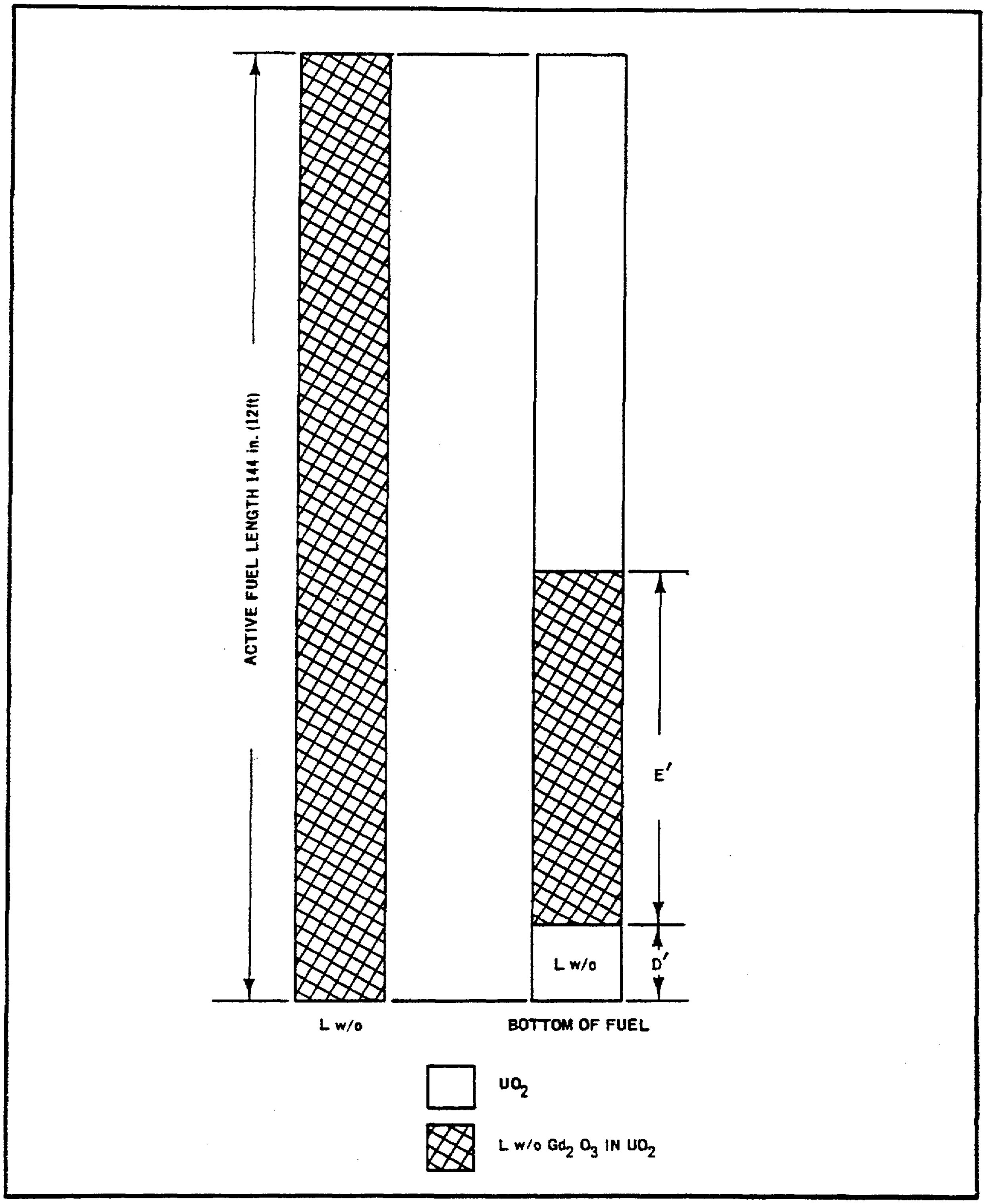

Figure 3-3. Axial Gadolinium Distribution for Bundle Type 3 of Figure 3-1

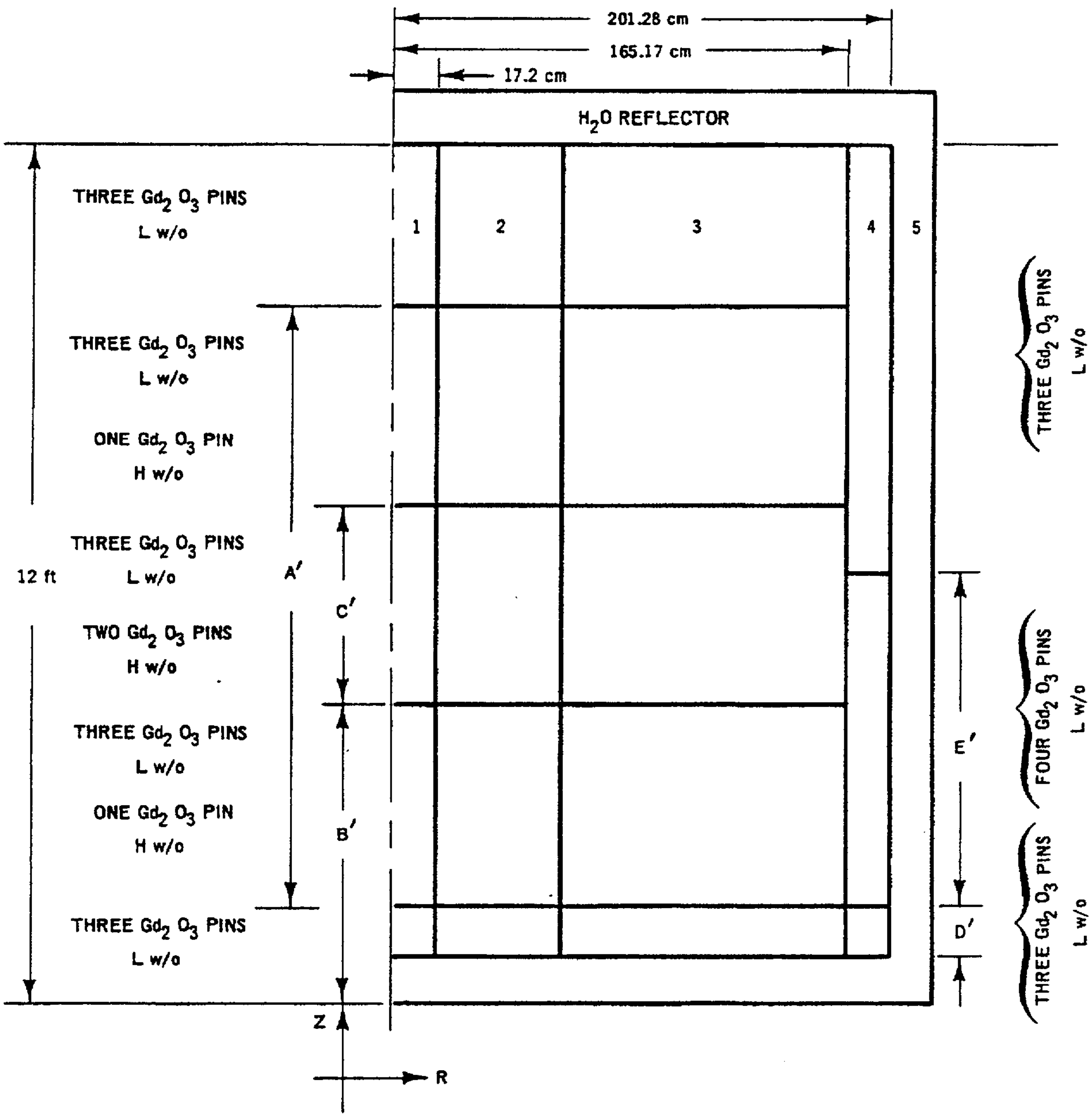

REGION	DESCRIPTION
1	THE RADIUS IS EQUIVALENT TO THAT OF AN EQUIVALENT CRUCIFORM CONTROL ROD FOUR–BUNDLE CELL
2	UNCONTROLLED FUEL. THE RADIUS OF THIS REGION IS DETERMINED BY THE ROD WORTH
3 & 4	PARTIALLY CONTROLLED FUEL. Σp IS DEPENDENT ON THE CONTROL ROD WORTH
5	30 cm OF H_2O REFLECTOR

Figure 3-4. Reactor Geometry for Analyzing Rod Drop Excursion

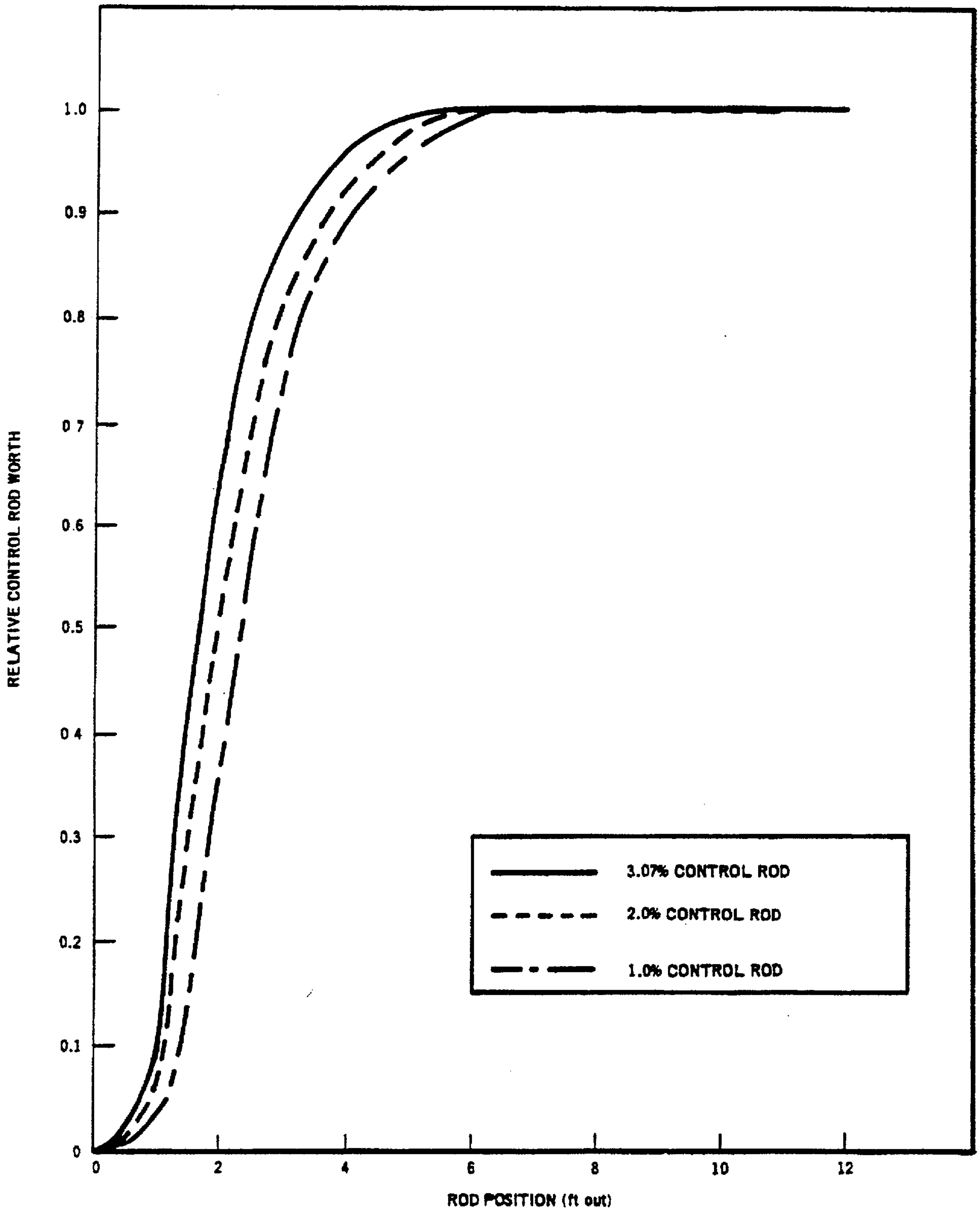

Figure 3-5. Relative Control Rod Worth for Rod Drop Excursion at 20°C

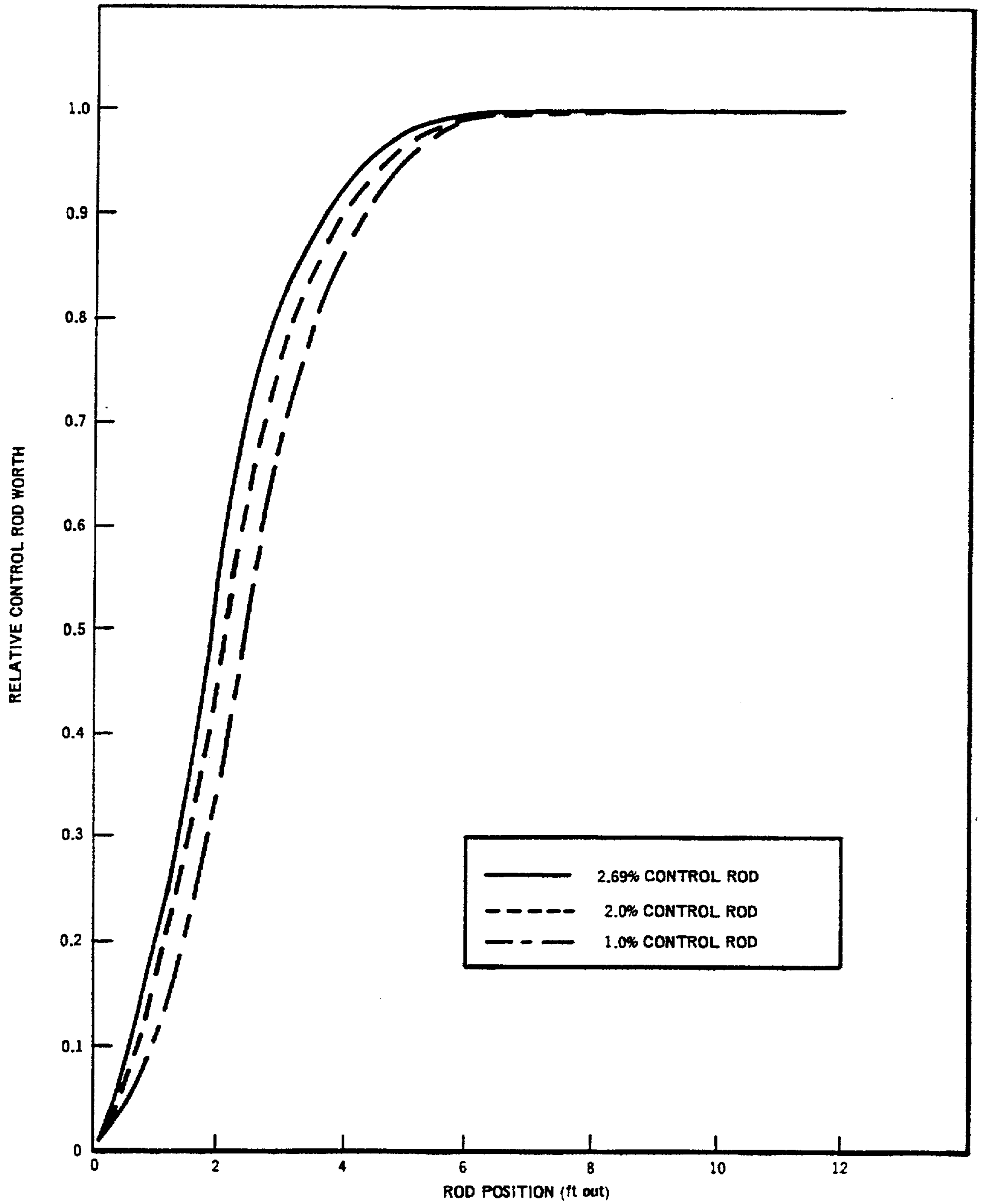

Figure 3-6. Relative Control Rod Worth for Rod Drop Excursion at 286°C

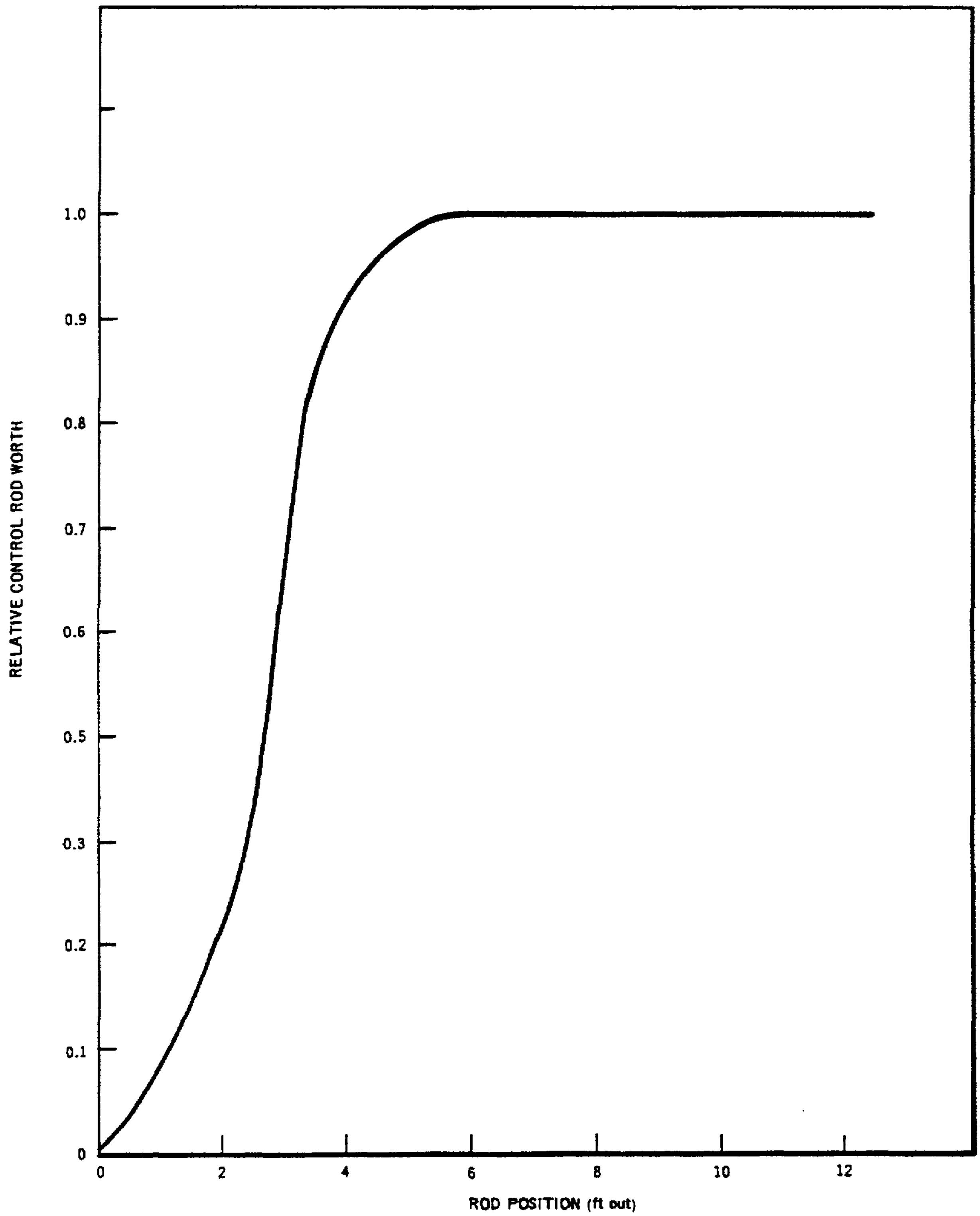

Figure 3-7. Relative Control Rod Worth for Rod Drop Excursion at 10% Power for a 2.0% Control Rod at BOL

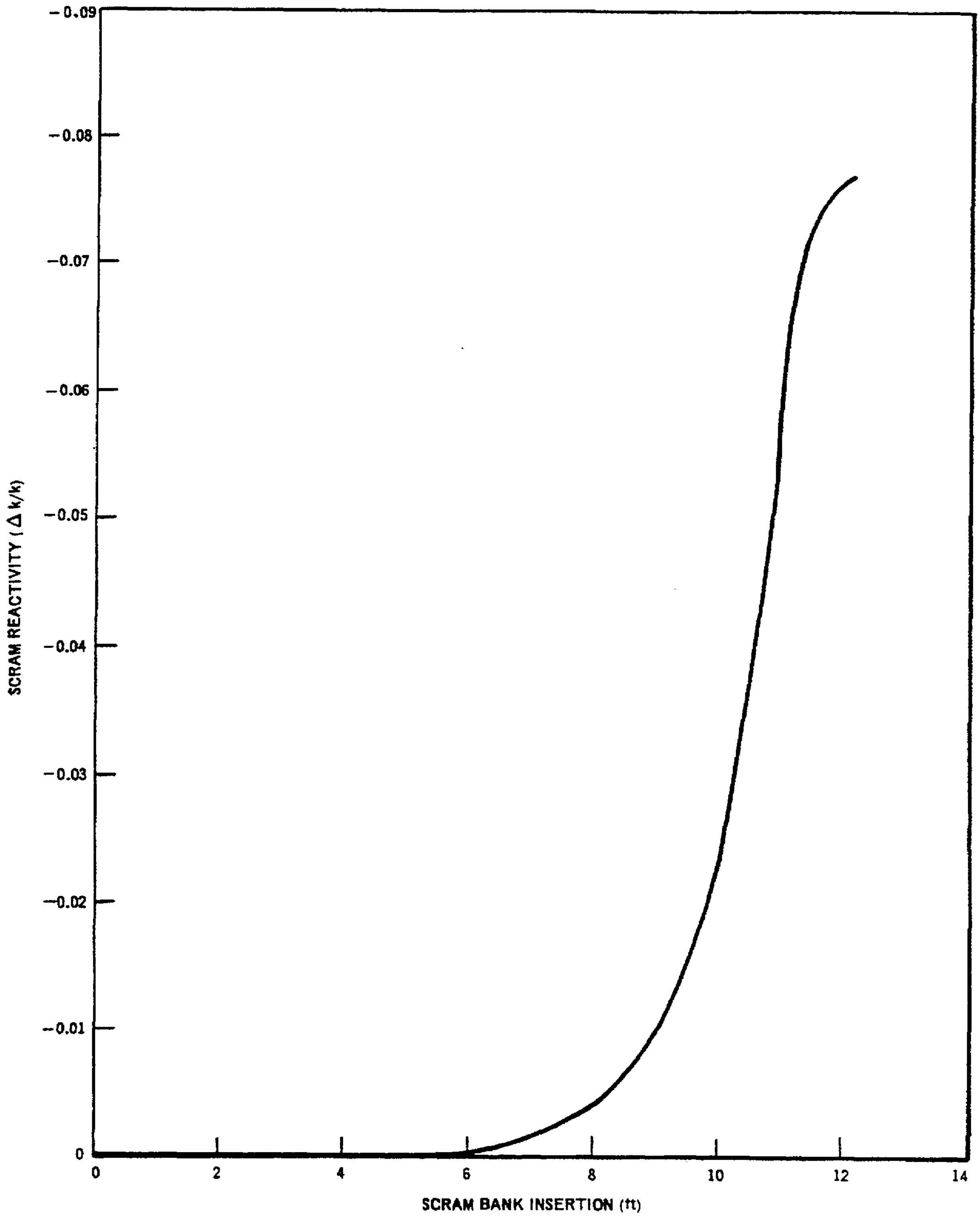

Figure 3-8. Scram Reactivity Function for the Cold Startup Reactor State

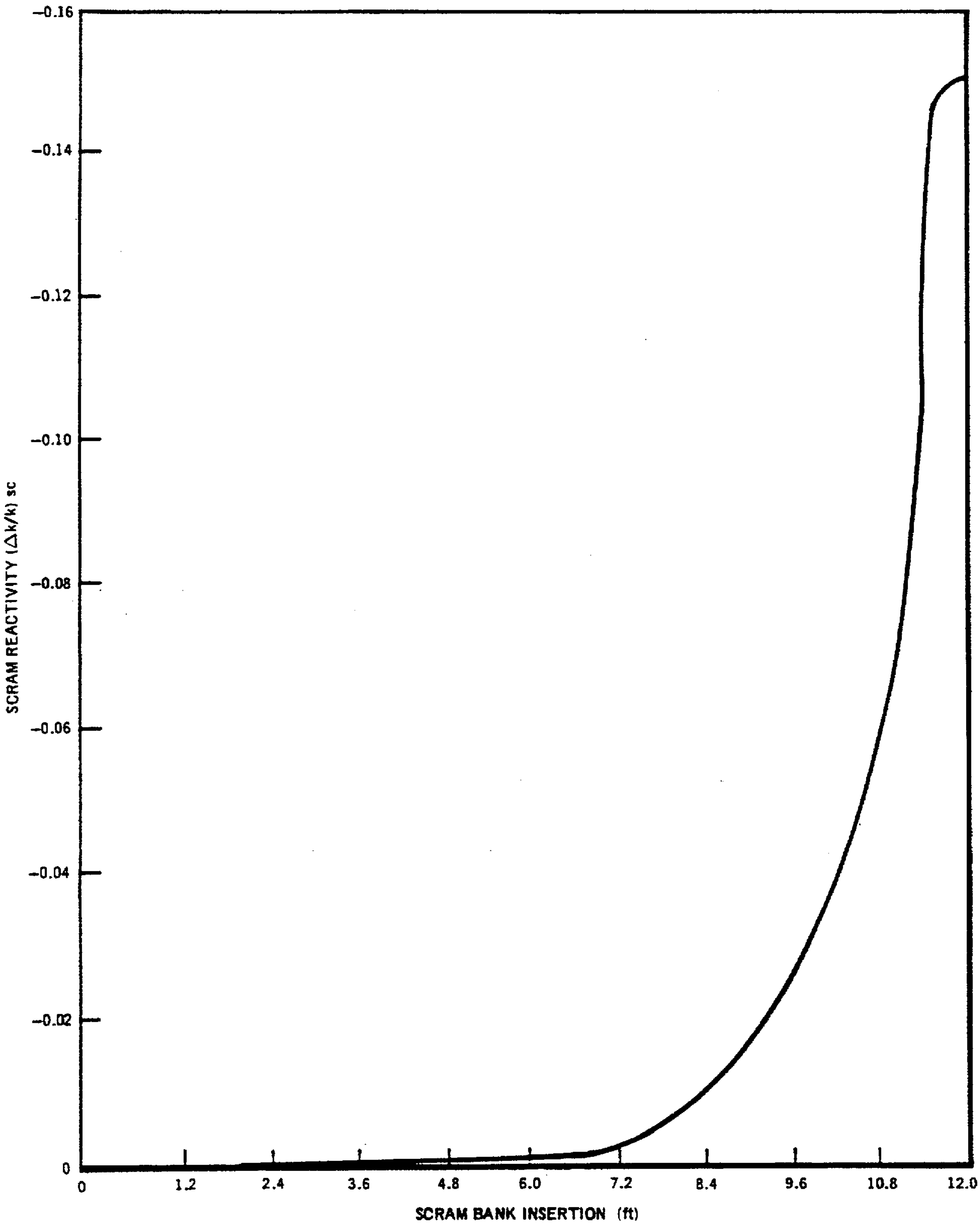

Figure 3-9. Scram Reactivity Function for the Hot Startup Reactor State

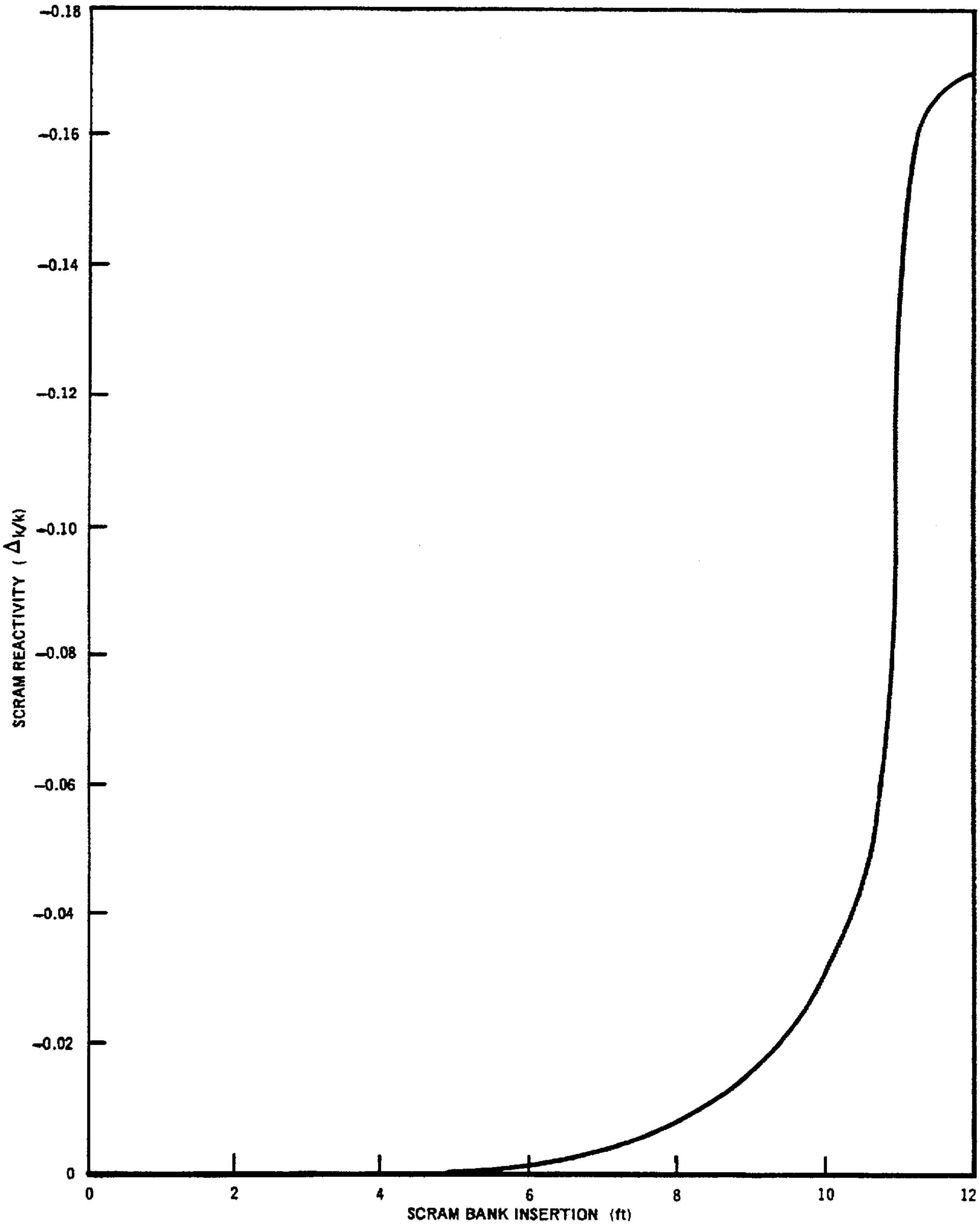

Figure 3-10. Scram Reactivity Function for 10% Power

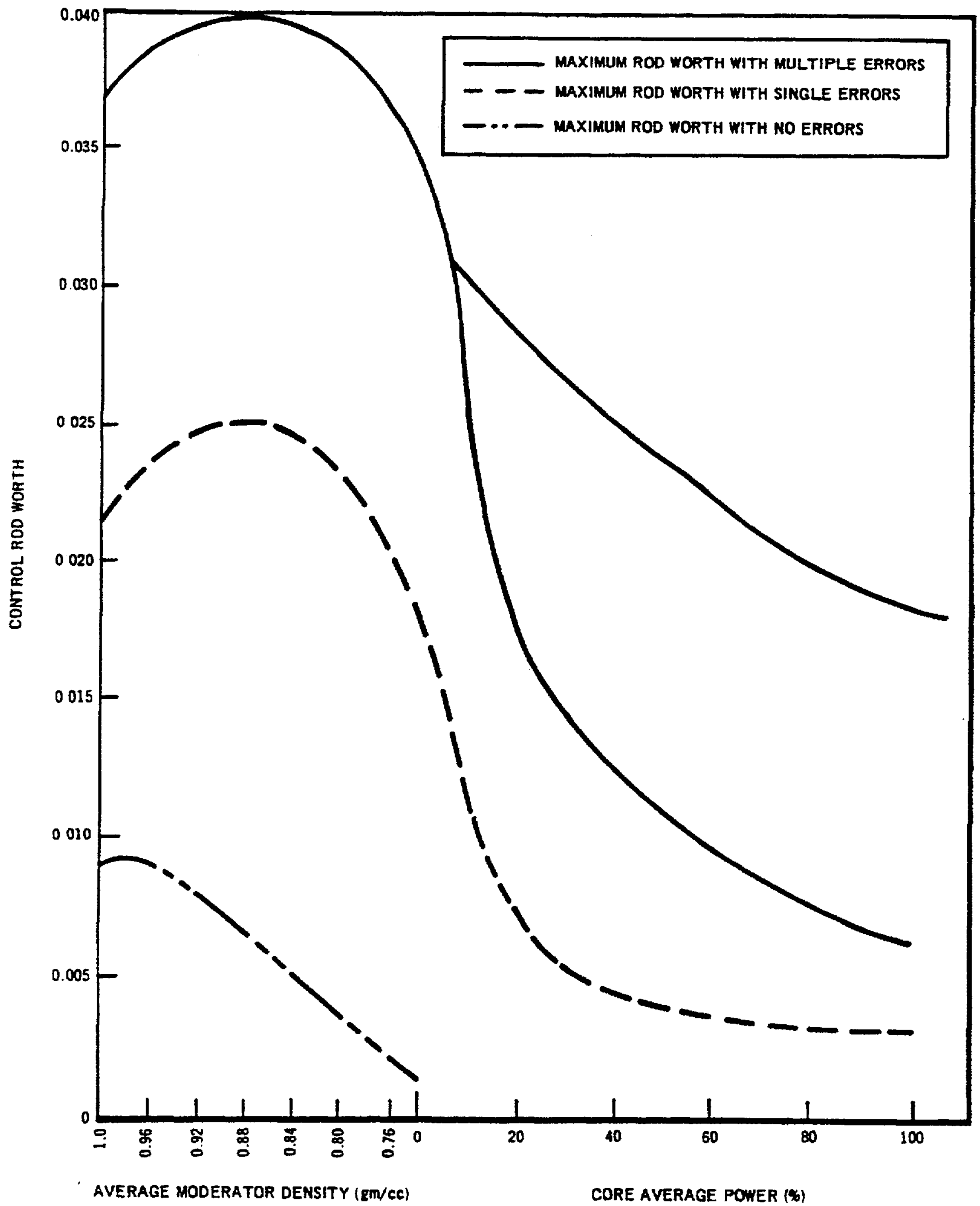

Figure 3-11. Maximum Control Rod Worth for Various Normal and Abnormal Operating States at the Most Reactive Point in Core Life (6500 MWd/T)

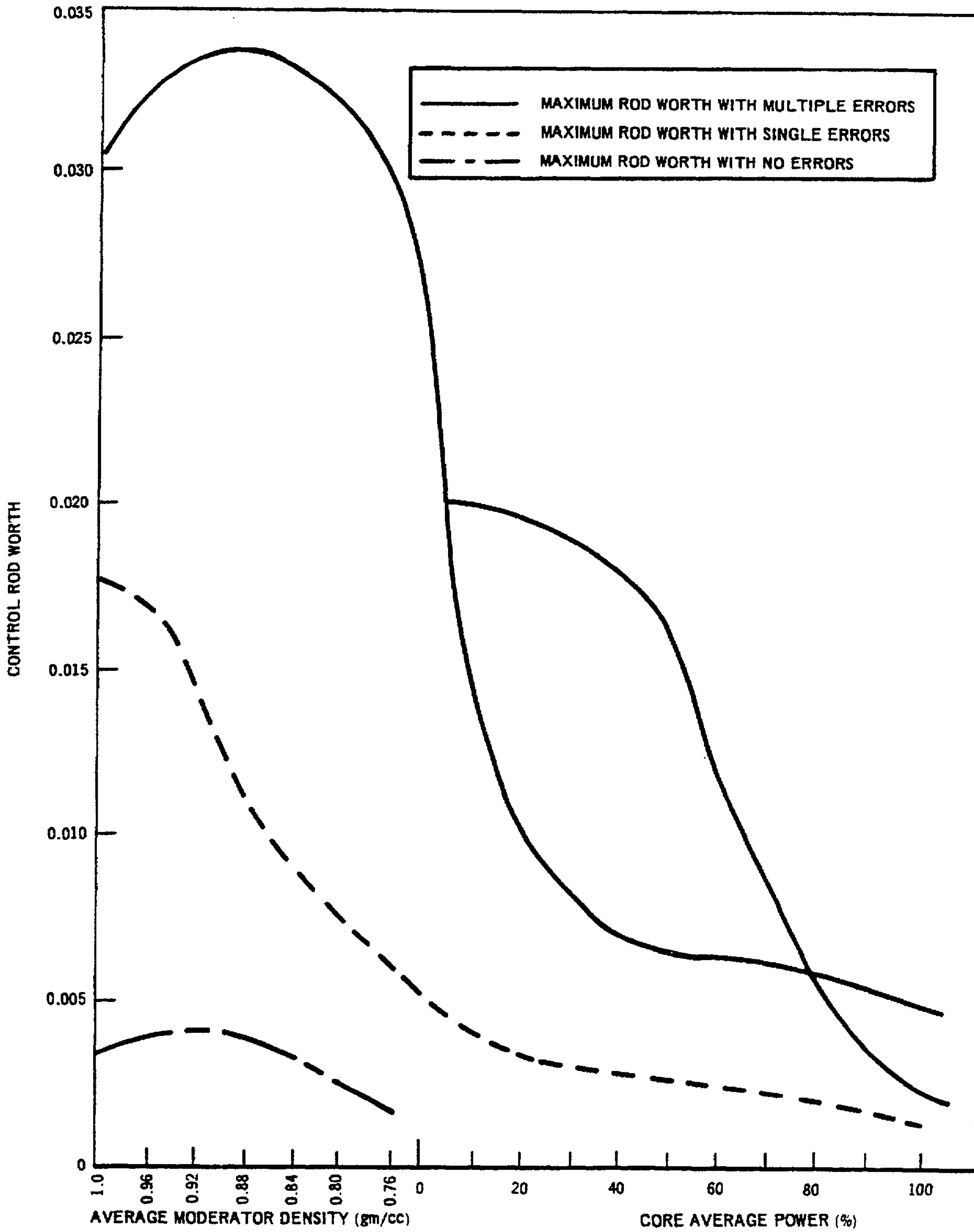

Figure 3-12. Maximum Control Rod Worth for Various Normal and Abnormal Operating States at Begining of Life

REFERENCES

1. Stirn, R. C., et al., *Rod Drop Accident Analysis for Large Boiling Water Reactors,* March 1972, (NEDO-10527).

2. Brown's Ferry FSAR Amendment No. 21, Figures 3.6-5 and 3.6-6.